*Astronomy & Astrophysics* manuscript no.
(will be inserted by hand later)

arXiv:astro-ph/0104053v1 3 Apr 2001

# Lithium abundances for 185 main-sequence stars [*]

## Galactic evolution and stellar depletion of lithium

Y.Q. Chen[1,2], P.E. Nissen[2], T. Benoni[2], and G. Zhao[1]

[1] Beijing Astronomical Observatory, Chinese Academy of Sciences, Beijing 100012, P R China
e-mail: `cyq@yac.bao.ac.cn`
[2] Institute of Physics and Astronomy, University of Aarhus, DK–8000 Aarhus C, Denmark
e-mail: `pen@ifa.au.dk`

Received 9 January 2001 / Accepted 7 March 2001

**Abstract.** We present a survey of lithium abundances in 185 main-sequence field stars with $5600 \lesssim T_{\rm eff} \lesssim 6600$ K and $-1.4 \lesssim$ [Fe/H] $\lesssim +0.2$ based on new measurements of the equivalent width of the $\lambda 6708$ Li I line in high-resolution spectra of 130 stars and a reanalysis of data for 55 stars from Lambert et al. (1991). The survey takes advantage of improved photometric and spectroscopic determinations of effective temperature and metallicity as well as mass and age derived from Hipparcos absolute magnitudes, offering an opportunity to investigate the behaviour of Li as a function of these parameters. An interesting result from this study is the presence of a large gap in the $\log\varepsilon({\rm Li}) - T_{\rm eff}$ plane, which distinguishes 'Li-dip' stars like those first identified in the Hyades cluster by Boesgaard & Tripicco (1986) from other stars with a much higher Li abundance. The Li-dip stars concentrate on a certain mass, which decreases with metallicity from about 1.4 $M_\odot$ at solar metallicity to 1.1 $M_\odot$ at [Fe/H] $\simeq -1.0$. Excluding the Li-dip stars and a small group of lower mass stars with $T_{\rm eff} < 5900$ K and $\log\varepsilon({\rm Li}) < 1.5$, the remaining stars, when divided into four metallicity groups, may show a correlation between Li abundance and stellar mass. The dispersion around the $\log\varepsilon({\rm Li})$ –mass relation is about 0.2 dex below [Fe/H] $\simeq -0.4$ and 0.3 dex above this metallicity, which cannot be explained by observational errors or differences in metallicity. Furthermore, there is no correlation between the residuals of the $\log\varepsilon({\rm Li})$-mass relations and stellar age, which ranges from 1.5 Gyr to about 15 Gyr. This suggests that Li depletion occurs early in stellar life and that other parameters than stellar mass and metallicity affect the degree of depletion, e.g. initial rotation velocity and/or the rate of angular momentum loss. It cannot be excluded, however, that a cosmic scatter of the Li abundance in the Galaxy at a given metallicity contributes to the dispersion in Li abundance. These problems make it difficult to determine the Galactic evolution of Li from the data, but a comparison of the upper envelope of the distribution of stars in the $\log\varepsilon({\rm Li})$ – [Fe/H] plane with recent Galactic evolutionary models by Romano et al. (1999) suggests that novae are a major source for the Li production in the Galactic disk; their occurrence seems to be the explanation of the steep increase of Li abundance at [Fe/H] $\simeq -0.4$.

**Key words.** Stars: abundances – Stars: evolution – Stars: late-type – Galaxy: evolution – Galaxy: solar neighbourhood

## 1. Introduction

Following the discovery by Spite & Spite (1982) of a uniform abundance of lithium in unevolved halo stars with $T_{\rm eff} > 5700$ K, this trace element has attracted much attention, and many papers have addressed problems of Galactic evolution and stellar depletion of Li. The diagram of Li abundance versus metallicity for F and G stars illustrates these problems. Below [Fe/H] $\simeq -1.4$ one sees a lithium plateau with a very small dispersion of the Li abundance (e.g. Spite et al. 1996) and perhaps a slight slope of Li vs. [Fe/H] (Ryan et al. 1999). Above [Fe/H] $\simeq -1.4$ the upper envelope of the distribution of stars in the $\log\varepsilon({\rm Li})$ – [Fe/H] diagram increases from the plateau value $\log\epsilon\,({\rm Li}) \simeq 2.2$ to about 3.0 at [Fe/H] $\simeq 0.0$ (Lambert et al. 1991). In the same metallicity range the Li abundances show, however, an enormous variation at a given metallicity, i.e. more than 3 dex.

The prevalent interpretation of the $\log\varepsilon({\rm Li})$ – [Fe/H] diagram is that the plateau represents the primordial Big Bang $^7$Li abundance and that the upper envelope of the distribution reflects the Galactic evolution of lithium.

---

*Send offprint requests to*: P.E. Nissen

[*] Based on observations carried out at Beijing Astronomical Observatory (Xinglong, P R China) and European Southern Observatory, La Silla, Chile

Before adopting this explanation we should, however, be able to explain why stars with [Fe/H] $\gtrsim -1.4$ has such a large dispersion of their Li abundances. Furthermore, it is not clear if stars along the upper envelope have retained their original Li abundances or suffered a mild degree of Li depletion. One may also ask if there has been a homogeneous evolution of Li in the Galaxy as a function of [Fe/H] or if there is a dispersion of the Li abundance in the interstellar medium at a given metallicity related to time or position in the Galaxy.

In an interesting paper on Li abundances in 81 dwarf stars, Lambert et al. (1991) discovered that dwarf stars with $5900 < T_{\rm eff} < 6600$ K tend to have a bimodal distribution in the $\log \varepsilon$(Li)–$T_{\rm eff}$ diagram (see their Fig. 4). Stars belonging to a 'high-Li' group show an increasing abundance of Li with $T_{\rm eff}$ and [Fe/H]. Most of the stars in the 'low-Li' group seem to have evolved from $T_{\rm eff}$(ZAMS) $\simeq 6600$ K, i.e. the temperature of the 'Li-dip' stars discovered in the Hyades by Boesgaard & Tripicco (1986), but a few low-Li stars have no connection to the Li-dip. Still, they have an order of magnitude less lithium than stars in the high-Li group with corresponding parameters $T_{\rm eff}$, $M_V$, and [Fe/H].

In a comprehensive work on Li abundances of slightly evolved F-type disk stars, Balachandran (1990) also identified a number of Hyades dip-like field stars, which all appear to have evolved from a $T_{\rm eff}$(ZAMS) range of 6500 to 6800 K despite of their metallicity differences. As pointed out by Balachandran this means that the characteristic mass of the Li-dip stars decreases with metallicity.

Recently, Romano et al. (1999) have studied the Galactic evolution of Li by comparing the distribution of stars in the $\log \varepsilon$(Li) – [Fe/H] diagram with predictions from chemical evolution models that include several sources of $^7$Li production. From a compilation of literature data they suggest that the Li plateau extends up to [Fe/H] $\simeq -0.5$ with a steep rise of the Li abundance for higher metallicities. In order to reproduce this trend, novae have to be included as a dominant contributor to the Li production in the Galaxy in addition to the contribution from AGB stars, Type II SNe and cosmic ray processes.

In order to verify and extend the interesting findings of Balachandran (1990), Lambert et al. (1991) and Romano et al. (1999), we have measured the equivalent width of the Li I $\lambda$6708 line in 133 main seqeuence field stars with $5600 \lesssim T_{\rm eff} \lesssim 6600$ K and $-1.4 \lesssim$ [Fe/H] $\lesssim +0.2$. Li abundances have been derived from a model atmosphere analysis of the data, and stellar masses and ages have been derived from a comparison of $T_{\rm eff}$, $M_V$ values with stellar evolutionary tracks in the HR diagram using Hipparcos parallaxes to determine the absolute magnitudes of the stars. Furthermore, the Lambert et al. (1991) data have been analyzed in the same way. The resulting large homogeneous set of Li abundances is used to rediscuss the distribution of stars in the $\log \varepsilon({\rm Li}) - T_{\rm eff}$ and $\log \varepsilon({\rm Li}) - $ [Fe/H] diagrams aiming at a better understanding of the Galactic evolution of lithium and the depletion in stars.

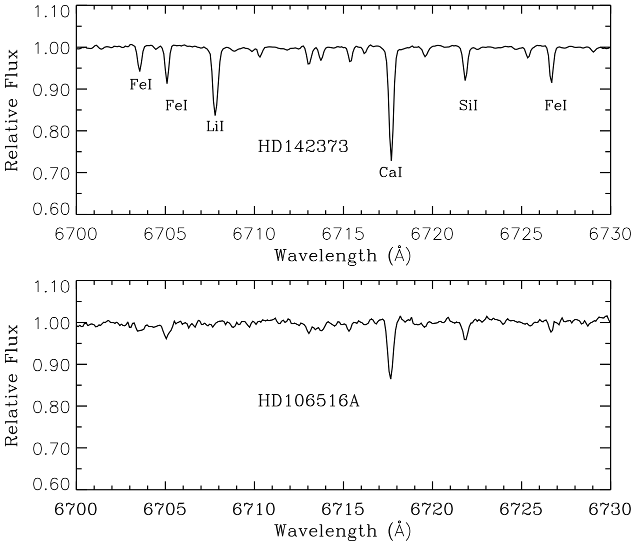

**Fig. 1.** Representative Xinglong spectra in the region of the Li I $\lambda$6708 line for HD 142373 ($T_{\rm eff} = 5920$ K, $\log g = 4.27$, [Fe/H] $= -0.39$ and a high $S/N \sim 400$) with a quite strong lithium line and HD 106516A ($T_{\rm eff} = 6135$ K, $\log g = 4.34$, [Fe/H] $= -0.71$ and a relatively low $S/N \sim 160$) without Li detection.

## 2. Observations and data reductions

The primary set of Li I $\lambda$6708 equivalent widths was obtained from CCD spectra of 90 main-sequence stars with $5700 < T_{\rm eff} < 6600$ K and $-1.0 <$ [Fe/H] $< +0.1$ observed with the Coudé Echelle Spectrograph at the 2.16m telescope of Beijing Astronomical Observatory; see Chen et al. (2000), who have used these spectra in connection with a large survey of abundances of heavier elements in F and G disk dwarfs. The spectra cover the region 5500 - 9000 Å at a resolution of 40 000 and have $S/N$ above 150; see Fig. 1.

The second set of equivalent widths was measured in spectra of 28 dwarfs with $5500 < T_{\rm eff} < 6500$ K and $-1.4 <$ [Fe/H] $< -0.5$ observed with the ESO NTT EMMI echelle spectrograph at a resolution of 60 000 and $S/N \gtrsim 150$. These spectra have previously been used by Nissen & Schuster (1997) in a study of the chemical composition of halo and disk stars with overlapping metallicities.

The third sample consists of 15 turnoff stars with $-0.8 <$ [Fe/H] $< +0.2$. They were observed in the Li I line region with the ESO 1.4m CAT telescope and the CES spectrograph at a resolution of 105 000 and a very high $S/N$ of 300 to 1000. These spectra were primarily obtained for a study of the lithium isotope ratio and some of them have been analyzed by Nissen et al. (1999), who detected $^6$Li in two stars (HD 68284 and HD 130551) at a level corresponding to $^6{\rm Li}/^7{\rm Li} \simeq 0.05$. Here we use the equivalent width of the Li I line to derive the total Li abundance of the stars.

Due to the complications by measuring reliable equivalent widths and making a proper model atmosphere anal-

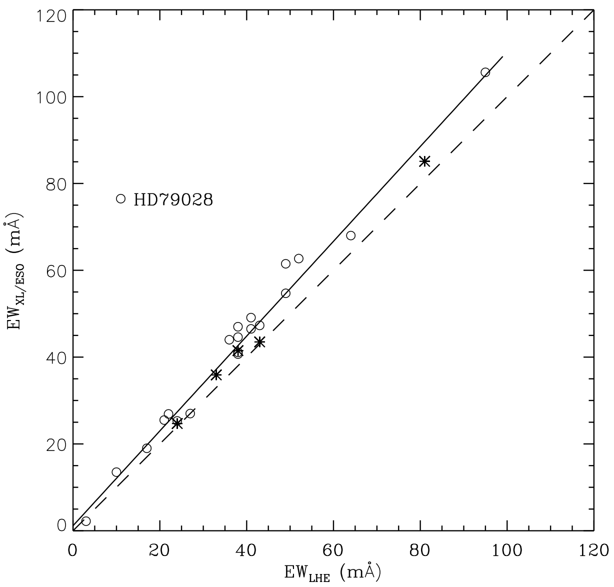

**Fig. 2.** Equivalent widths of the Li I λ6708 line measured from Xinglong (open circles) or ESO (asterisks) spectra compared to equivalent widths given by Lambert et al. (1991).

ysis of double-lined spectroscopic binaries such stars were excluded from the three samples. Proven or suspected single-lined spectroscopic binaries were, however, retained. According to Chen et al. (2000) such stars do not appear to have any abundance anomalies of the heavier elements. As discussed later there are, however, indications that the Li abundance may be peculiar for such SB1 stars.

The spectra were reduced using standard MIDAS (Xinglong data) and IRAF (ESO data) routines for order definition, background correction, flatfielding, extraction of echelle orders, wavelength calibration and continuum fitting. At the resolution of the Xinglong and ESO NTT spectra, the profile of the Li I doublet is well approximated by a Gaussian function despite of its inherent asymmetry. Hence, the equivalent width of the Li I line was measured by Gaussian fitting, which has the advantage that the weak Fe I λ6707.44 line in the blue wing of the Li line gives no significant contribution. For the high resolution, high $S/N$ spectra from the ESO CES the equivalent width was measured both by Gaussian fitting and by direct integration excluding the blending Fe I line. The two sets of data agree within ±1 mÅ.

Lambert et al. (1991) measured their equivalent widths from spectra obtained at McDonald Observatory with the Coudé Spectrographs of the 2.1 and 2.7m telescopes. The resolution of these spectra is around 35 000 and $S/N \sim 150$. Twenty stars are in common with the Xinglong sample and 5 stars with the ESO sample. A comparison of the equivalent widths is shown in Fig. 2. Obviously, Lambert et al.'s EWs are systematically lower than the Xinglong and ESO data. The reason for this discrepancy is unclear. A linear least square fit gives

$$EW_{\rm XL} = 1.09\,(\pm 0.03)\,EW_{\rm LHE} + 1.12\,(\pm 1.26)\ \ (m\text{Å}) \qquad (1)$$

where the deviating star HD 79028 has been been excluded from the regression. We suspect that this star was misidentified by Lambert et al. because there is a very good agreement between Xinglong EWs measured by Chen et al. (2000) and those of Edvardsson et al. (1993) for 26 metal lines in common.

The relation between the Lambert et al. equivalent widths and those based on the Xinglong and ESO spectra appears to be well defined; the rms scatter around the line shown in Fig. 2 is less than 3 mÅ (excluding HD 79028). Hence, we have rescaled the Lambert et al. data according to Eq. 1 to get a homogeneous set of equivalent widths of Li I λ6708.

## 3. Analysis

Effective temperatures were determined from the Strömgren $(b-y)$ color index using the calibration of Alonso et al. (1996). For the large majority of stars the gravities were determined via Hipparcos parallaxes (ESA 1997) as described by Chen et al. (2000). For the more distant stars we adopt a spectroscopic gravity obtained by requiring that Fe I and Fe II lines provide the same iron abundance. Metallicities were taken from Chen et al. (2000), Nissen & Schuster (1997), and Edvardsson et al. (1993). For a few stars not included in these sources, [Fe/H] was derived from the equivalent widths of the λ6703 and λ6705 Fe I lines given by Lambert et al. using "solar" oscillator strengths. Microturbulences were taken from Chen et al. (2000) or calculated from the empirical relation found by Edvardsson et al. (1993). The uncertainties of the parameters are: $\sigma(T_{\rm eff}) = 70$ K, $\sigma(\log g) = 0.1$ dex, $\sigma([{\rm Fe/H}]) = 0.1$ and $\sigma(\xi) = 0.3$ km s$^{-1}$.

The model atmospheres were interpolated from a grid of plane-parallel, LTE models computed with the MARCS code by Bengt Edvardsson (Uppsala). The corresponding analysis program, SPECTRUM, was used to calculate equivalent widths of the Li I line as a function of the Li abundance with wavelengths and oscillator strengths of the Li doublet components taken from Sansonetti et al. (1995) and Yan & Drake (1995), respectively (see Smith et al. 1998, Table 3). The contribution of the $^6$Li isotope was assumed to be negligible. Li abundances were then obtained by requiring that the theoretical equivalent widths should match the observed ones.

The uncertainty in the Li abundance, resulting from errors of the equivalent widths, is around 0.05 dex for stars with EW ∼ 10-120 mÅ increasing rapidly for stars with weaker lines. Changes of the Li abundance due to errors in the model atmosphere parameters are 0.058 dex for $\Delta T = +70$ K, −0.001 dex for both $\Delta \log g = +0.1$ and $\Delta[{\rm Fe/H}] = +0.1$, −0.002 for $\Delta\xi_t = +0.3$ km s$^{-1}$. These numbers were derived for HD 142373 with $T_{\rm eff} = 5920$ K, $\log g = 4.27$, $[{\rm Fe/H}] = -0.39$ and a Li I equivalent width of 49 mÅ, but are representative for the whole sample. For the Lambert et al. sample our derived Li abundances agree with their original values and those derived by Romano et al. (1999) within 0.1 dex. The differences are mainly due to different ways of determining $T_{\rm eff}$ and our rescaling of the EWs published by Lambert et al.

Finally, non-LTE corrections were applied to the derived Li abundances based on the work by Carlsson et al. (1994), who studied non-LTE formation of the Li I $\lambda$6708 line as a function of effective temperature, gravity, metallicity and Li abundance. For the present sample of stars, the largest correction (LTE − non-LTE) is 0.12 dex for the hottest and most Li-rich stars; the correction decreases with temperature and becomes slightly negative for the cool Li-poor stars.

Atmospheric parameters and Li abundances are presented in Table 1, which also includes the absolute magnitude derived from the Hipparcos parallax (ESA 1997). In a few cases where the Hipparcos parallax is not available or has a low relative accuracy the Strömgren $c_1$ index has been used to determine $M_V$ (see Edvardsson et al. 1993). Stellar masses and ages derived from evolutionary tracks of VandenBerg et al. (2000) (see Sect. 4.2) are also given in Table 1.

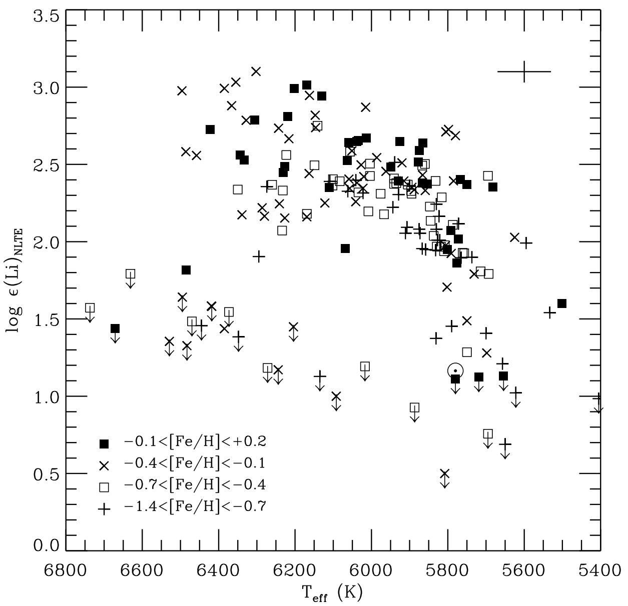

**Fig. 3.** Lithium abundance versus effective temperature for stars in the present survey. Upper limits of the Li abundance are indicated with downward directed arrows.

## 4. Discussion

### 4.1. Li vs. effective temperature

Fig. 3 shows the Li abundance vs. $T_{\rm eff}$ for all stars in the present survey. As seen, the stars tend to separate into two groups, one with high and one with low Li abundances. Although there is a significant spread of the Li abundance within each group, a gap of at least 1.0 dex is seen for $T_{\rm eff} > 5900$ K suggesting that a special and very rapid Li-depletion mechanism is operating in the interior of the low-Li stars.

In the low-Li group almost all abundances derived are upper limits, and the apparent linear correlation between the Li abundance and $T_{\rm eff}$ simply reflects the observational detection limit, EW$\simeq$ 3 mÅ, which corresponds to a Li abundance of 1.0 dex at $T_{\rm eff} = 5800$ K, 1.3 dex at $T_{\rm eff} = 6200$ K and 1.6 dex at $T_{\rm eff} = 6600$ K. As discussed in the next section, most of the low-Li stars with $T_{\rm eff} > 5900$ K have evolved from an effective temperature range corresponding to that of the Hyades Li-dip stars.

In the high-Li region, there is a spread of 1.0 dex in Li abundance at a given $T_{\rm eff}$. Metallicity seems to be responsible for the main part of the scatter based on the fact that the upper envelope consists of stars with [Fe/H] $> -0.4$, while nearly all stars with [Fe/H] $< -0.4$ have a Li abundance lower than 2.5 dex. This result, coupled with the fact that there is no large Li abundance differences among stars with $-1.4 <$ [Fe/H] $< -0.6$ and $T_{\rm eff} > 5900$ K, suggests a significant increase of the Galactic production of lithium around [Fe/H] $\sim -0.4$.

In the $T_{\rm eff} > 5900$ K range, the mean Li abundance of stars in the high-Li region shows a decrease with temperature for [Fe/H] $> -0.4$ while it is nearly $T_{\rm eff}$ independent for [Fe/H] $< -0.4$. In both metallicity groups a steep decline of the Li abundance begins at $T_{\rm eff} \simeq 5900$ K. Furthermore, a large scatter in Li abundance is apparent in the range $5600 \lesssim T_{\rm eff} \lesssim 5900$ with a tendency of a bimodal distribution. The Sun with a Li abundance of $\log \varepsilon({\rm Li}) = 1.16$ (Steenbock & Holweger 1984) belongs to the low-Li group.

### 4.2. Stellar masses and ages

In order to study the behaviour of Li as a function of stellar mass and age, the positions of the stars in the $M_V - \log T_{\rm eff}$ diagram were compared to the evolutionary tracks of VandenBerg et al. (2000). Masses and ages were derived as described by Chen et al. (2000). The typical error of the mass is 0.03-0.06 $M_\odot$. For most of the stars the age could be determined with an error of 15-20 %, but a number of stars situated close to the ZAMS or in the hook region of the evolutionary tracks have much larger age errors. For these stars no age is given in Table 1.

Fig. 4 shows the position of the stars in the $M_V - \log T_{\rm eff}$ diagram for four metallicity ranges. In panel a), that contains the most metal rich stars, 46 Hyades stars are added. They were selected from the papers of Boesgaard & Tripicco (1986), Boesgaard & Budge (1988) and Thorburn et al. (1993) with the condition that they should lie in the same $T_{\rm eff}$ range as our program stars, and excluding known binaries. Strömgren photometry of the Hyades stars was taken from Crawford & Perry (1966) and Hipparcos parallaxes from Perryman et al. (1998). The effective temperatures were determined in the same way as for the program stars, and the derived (non-LTE)

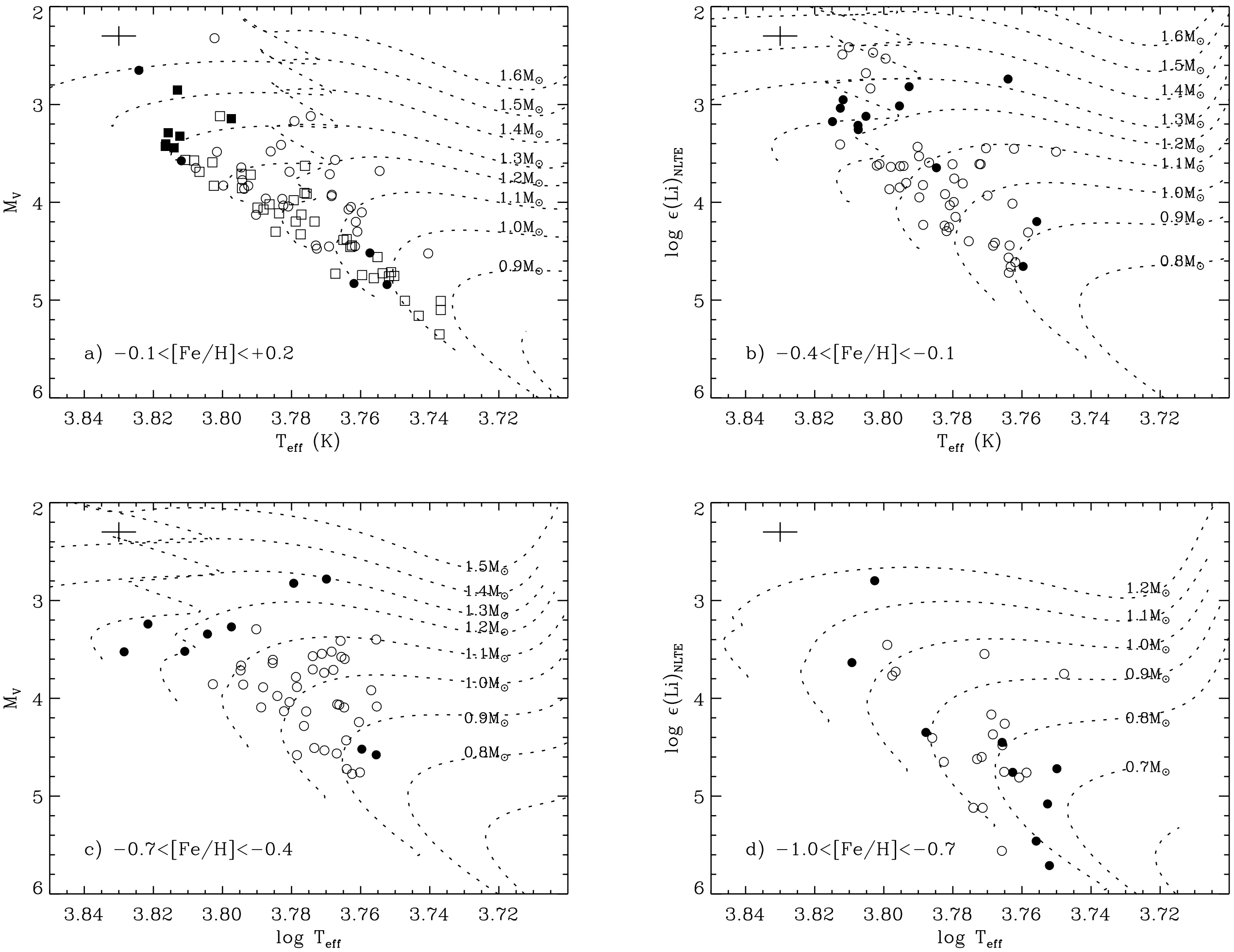

**Fig. 4.** Stellar positions in the $M_V$- log$T_{\rm eff}$ diagram divided according to metallicity and compared to evolutionary tracks of VandenBerg et al. (2000) corresponding to: **a**) [Fe/H] = +0.12, **b**) [Fe/H] = −0.20, **c**) [Fe/H] = −0.53, and **d**) [Fe/H] = −0.83. The filled circles indicate stars in the low-Li group and open circles stars in the high-Li group. In a) Hyades stars have been added and are plotted with squares instead of circles.

Li abundance is based on the Li-Fe blended EWs given in the three papers taking into account the contribution of the Fe I λ6707.44 blending line using log $gf = -2.29$ as derived from an analysis of the solar flux spectrum.

As seen from Fig. 4, stars in the low-Li region (filled circles) are concentrated either in the high mass or the low mass region at a given metallicity. The high-mass, low-Li stars probably suffer from the same depletion mechanism that acts on the Hyades. Like the Hyades Li-dip stars they are grouped in a quite narrow mass range. This is particular clear from panels b) and c). Furthermore, the mass of the Li-dip stars seems to be metallicity dependent with lower mass for the more metal-poor stars. According to Fig. 4, the critical mass is about $1.4 M_\odot$ at [Fe/H] $\simeq$ 0.1, $1.3 M_\odot$ at [Fe/H] $\simeq$ −0.20, $1.2 M_\odot$ at [Fe/H] $\simeq$ −0.5, and $1.1 M_\odot$ at [Fe/H] $\simeq$ −0.9. We also note that Li-dip stars can be found over a range of effective temperatures as clearly shown by panels b) and c), where stars with $T_{\rm eff} \sim 6600$ K and $T_{\rm eff} \sim 5700$ K both show the Li-dip depletion. Therefore, Li-dip stars in the field can not be distinguished by the temperature range alone. Instead, stellar mass is the key parameter that decides if a star suffers from the Li-dip depletion.

In the low-mass region there is a tendency that the lowest Li abundances occur among stars with the smallest masses, but there is no clear separation between high and low-Li stars. Apparently, the Li abundance is very sensitive to stellar mass and/or metallicity in this part of the HR diagram.

Two low-Li stars have intermediate masses, namely HD 80218 in panel b), and HD 106516A in panel d). HD 80218 was recently shown to be an astrometric binary by Gontcharov et al. (2000). HD 106516A (HR 4657) is a single-lined spectroscopic binary with an unusual large rotational velocity ($V$sini = 6.8 km s$^{-1}$, Fuhrmann & Bernkopf 1999) for its effective temperature ($T_{\rm eff}$= 6135 K) and metallicity ([Fe/H] = −0.71). Fuhrmann &

Bernkopf suggest that HD 106516A is a blue straggler and link the absence of Li to this special class of objects.

Lambert et al. (1991) also classified HD 106516A as a Li-poor star unrelated to both the Li-dip stars and the low-mass stars. They suggested six other stars as belonging to this 'intermediate-mass' group of Li-poor stars. None of these cases are, however, confirmed by our work. Based on the more accurate Hipparcos distances HD 95241 (HR 4285), HD 159332 (HR 6541) and HD 219476 clearly belong to the Li-dip stars. HD 30649 and HD 143761 (HR 5968) belong to the low-mass, Li-poor group. Finally, HD 79028 (HR 3648) is the star probably misidentified by Lambert et al. As discussed in Sect. 2, we measure a much larger equivalent width of the Li line, and hence the star belongs to the high-Li group. Altogether, we conclude that 'intermediate-mass' Li-poor stars are rare and may be binaries.

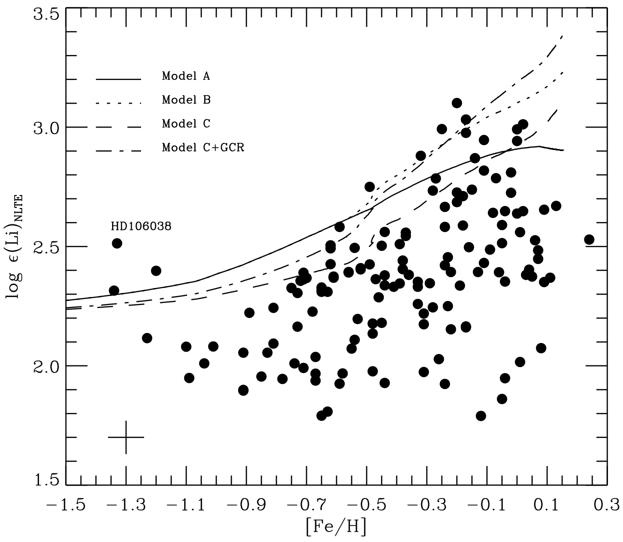

**Fig. 5.** Lithium abundances as a function of metallicity for stars in the high-Li group (see text for the definition). Theoretical predictions from Romano et al. (1999) are plotted.

### *4.3. Li vs. metal abundance*

In agreement with previous studies, a plot of $\log\varepsilon(\text{Li})$ as a function of [Fe/H] (see Fig. 5) indicates a large spread in Li abundance at a given metallicity, and the abundance range tends to increase with higher metallicity. The upper envelope of the distribution of $\log\varepsilon(\text{Li})$ for $[\text{Fe/H}] < -0.2$ is compatible with the the relation given by Lambert et al. (1991) as derived from the Rebolo et al. (1988) data. Above $[\text{Fe/H}] \simeq -0.2$ our sample is, however, not reaching such high Li abundances as the Rebolo et al. sample. This is partly due to the neglect of non-LTE correction by Rebolo et al., which leads to an overestimate of the Li abundance by about 0.1 dex for stars with the highest Li abundances. Furthermore, we note that stars with the highest Li abundances in this metallicity range in Rebolo et al. (1988) all have $T_{\text{eff}} > 6500$ K. These rather young, metal-rich stars are not represented in our sample of stars.

In order to show the upper envelope more clearly, Fig. 5 includes only stars belonging to the high-Li group defined as stars having $\log\varepsilon(\text{Li}) > 2.0$ for $T_{\text{eff}} > 5900$ K and $\log\varepsilon(\text{Li}) > 1.75$ for $T_{\text{eff}} \leq 5900$ K. As seen from Fig. 3 this definition excludes all Li-dip stars and the group of low-Li stars for $T_{\text{eff}} \leq 5900$ K.

The distribution of stars in Fig. 5 is compared to recent models for the Galactic evolution of Li by Romano et al. (1999). Their model A includes contributions to the Li production from low-mass AGB stars (C-stars), high-mass AGB stars and SNeII. As seen this model gives a very poor fit to the upper envelope. In model B, Li production by novae is included, which improves the fit at higher metallicities, but the models fails in predicting a too high Li abundance at metallicities around $[\text{Fe/H}] \sim -0.7$. Model C has no contribution from low-mass AGB stars and the yields of high-mass AGB stars and SNeII are reduced by a factor of two, whereas the contribution from novae is retained. This model provides a better fit of the upper envelope at low metallicities by predicting only a weak increase of the Li abundance from $[\text{Fe/H}] = -1.5$ to $-0.5$ and then a steep increase, but the model fails to account for the high Li abundance ($\sim 3.0$ dex) for stars with $-0.3 < [\text{Fe/H}] < -0.1$. Finally, model C+GCR also includes the contribution to Li production from cosmic ray processes. This model gives the best overall fit especially when one takes into account that all stars with $[\text{Fe/H}] > -0.1$ probably have suffered some Li depletion, as suggested by the high (3.3 dex) Li abundance in meteorites and in young stellar clusters like the Pleiades.

One low metallicity star (HD 106038 at $[\text{Fe/H}] = -1.33$ and $\log\varepsilon(\text{Li}) = 2.52$) lies well above the Li evolutionary curves, and also above the 'Spite plateau' for metal-poor halo stars. As shown by Nissen & Schuster (1997) this star has very peculiar abundances; $[\text{Si/Fe}] \simeq 0.6$, $[\text{Ni/Fe}] \simeq 0.2$, $[\text{Y/Fe}] \simeq 0.4$, and $[\text{Ba/Fe}] \simeq 0.5$. Most likely, the atmospheric composition of the star has been changed by mass transfer from an evolved component in its AGB phase causing the enrichment in Li and the *s*-process elements. The enrichment in Si and Ni is, however, difficult to explain.

### *4.4. Li vs. stellar mass and age*

It is evident from the $\log\varepsilon(\text{Li})$ – [Fe/H] diagram (Fig. 5) that only a few stars lie along the Li evolutionary curves predicted from the models of Romano et al. (1999). The canonical interpretation is that Li has been destroyed in the majority of the stars due to reactions with protons at the bottom of the outer convection zone of the star, i.e. at $T > 2.5\,10^6$ K. As the depth of the convection zone depends primarily on stellar mass a correlation between Li abundance and mass is then expected for a given metallicity. To investigate this, we have divided the high-Li stars

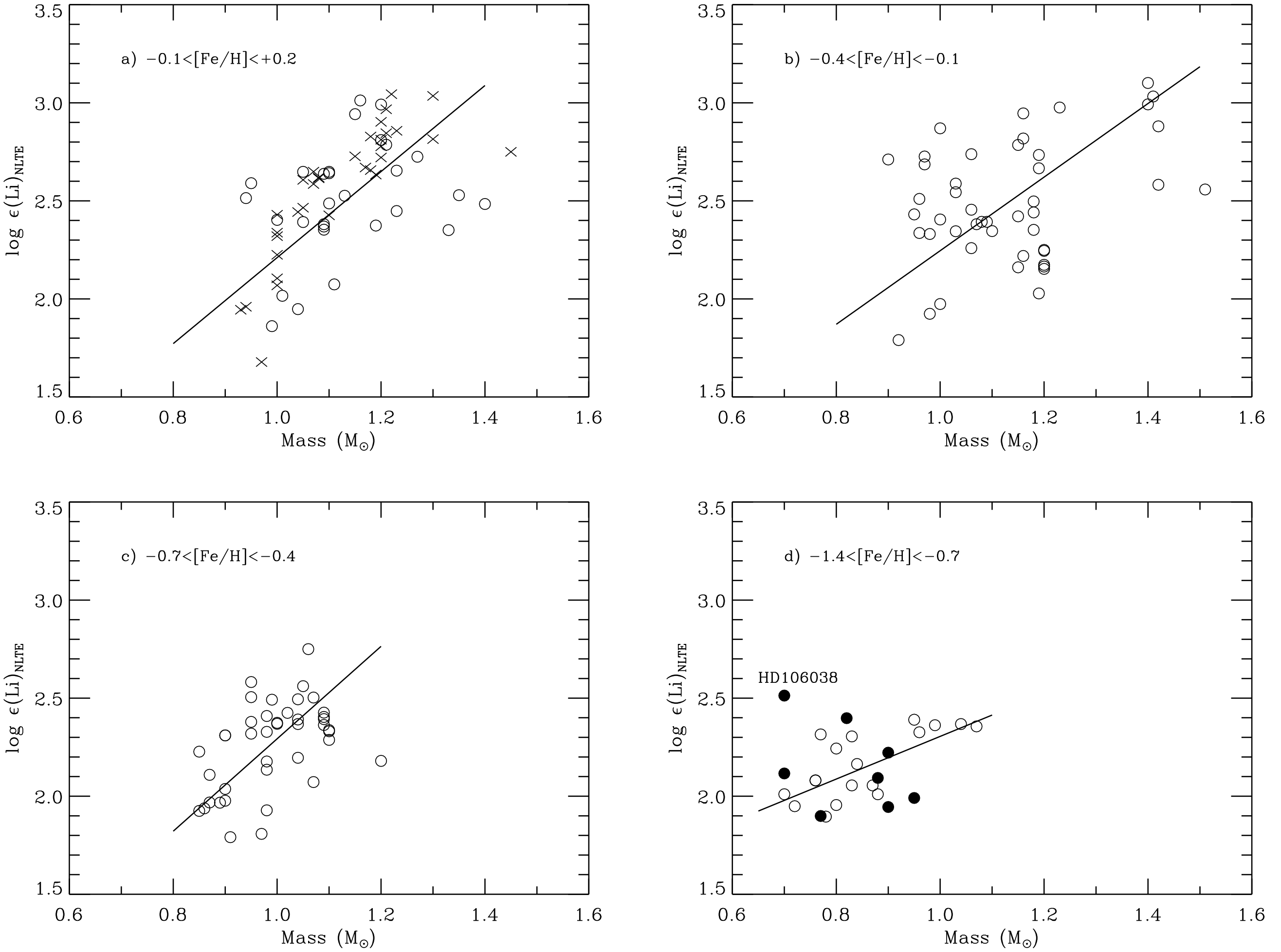

**Fig. 6.** Li abundance versus stellar mass for 'high-Li' stars divided into four metallicity groups. In **a)** Hyades stars outside the Li-dip have been added and are plotted with crosses. In **d)** stars with halo kinematics have been plotted with filled circles. The rest of the stars have disk kinematics.

(i.e. those included in Fig. 5) into four metallicity intervals and plotted the Li abundance as a function of mass (see Fig. 6). In panel a), Hyades stars outside the Li-dip region have been added.

As seen from Fig. 6 there may indeed be a correlation between Li abundance and mass. Excluding the Hyades and the peculiar star (HD 106038 straight lines have been fitted to the data taking into account errors in both coordinates. The slope of the fitted lines is about the same in panels a), b) and c), $\Delta \log \varepsilon(\mathrm{Li})/\Delta \mathrm{Mass} \simeq 2$. For the most metal-poor group, panel d), the slope is $\simeq 1$ but the correlation is marginal. It is also seen that the slope defined by the Hyades stars agrees well with that of the field stars and that the Hyades lie only slightly above the mean relation for the field stars despite of their younger age.

The dispersion around the fitted lines in Fig. 6 is, however, much larger than expected from the estimated errors of $\log \varepsilon(\mathrm{Li})$ and the stellar mass. From $\sigma \log \varepsilon(\mathrm{Li}) \simeq 0.10$ and $\sigma(\mathrm{Mass}) \simeq 0.05 M_\odot$ we would expect a dispersion in the $\log \varepsilon(\mathrm{Li})$ direction of 0.16 dex in panels a), b) and c) and 0.11 dex in panel d). The actual dispersion around the fitted lines is 0.32 dex in panels a) and b), 0.22 dex in c) and 0.14 dex in d). Furthermore, there is no significant correlation between the residuals of the fits and the stellar age (see Fig. 7) or the metallicity variation within each group. The most likely explanation is that the depletion of Li depends on other parameters than stellar mass, age and metallicity such as the initial rotational velocity of the star and/or the rate of angular momentum loss during its evolution. The same conclusion has been reached from studies of Li abundances of open cluster stars, e.g. the Hyades (Thorburn et al. 1993) and M67 (Jones et al. 1999) as well as from studies of Li abundances in upper main sequence stars (Balachandran 1990), solar-like stars (Pasquini et al. 1994) and subgiants (Randich et al. 1999).

The fact that there is no significant correlation between the residuals of the $\log \varepsilon(\mathrm{Li})$-mass relations and stellar age is interesting. As the age for the present sample of stars ranges from 1.5 Gyr to about 15 Gyr, the lack of correlation suggests that the main part of Li depletion occurs rather early in the stellar life, i.e. at ages $\lesssim 1.5$ Gyr. In a review of Li abundances in open cluster stars, Pasquini

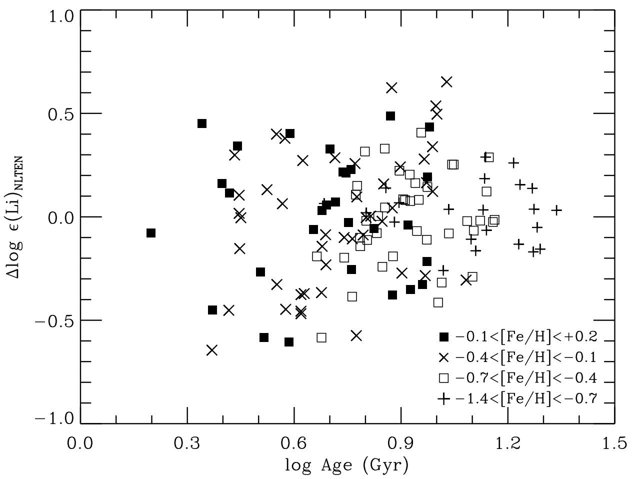

**Fig. 7.** The residuals of $\log\varepsilon$(Li) with respect to the $\log\varepsilon$(Li)-mass fits in Fig. 6 as a function of the logarithmic stellar age. The four metallicity groups are shown by different symbols.

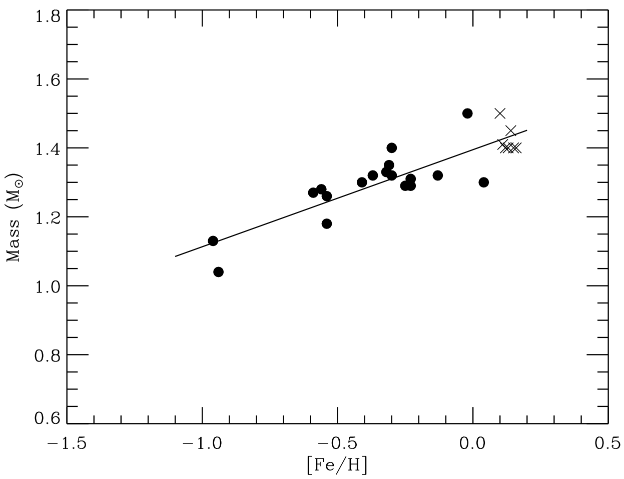

**Fig. 8.** The dependence of stellar mass on metallicity for Li-dip stars. Crosses refer to Hyades stars and filled circles to field stars.

(2000) reached a similar conclusion: most of the Li depletion occurs for stellar ages between $\sim 100$ and $\sim 600$ Myr.

There may, however, also be a contribution to the Li dispersion arising from a cosmic scatter of Li in the Galaxy at a given metallicity. To investigate this we have searched for correlations between Li abundances and stellar kinematics, but the outcome was negative. In the lowest metallicity group ($-1.4 <$ [Fe/H] $< -0.7$) eight stars have halo kinematics, i.e. elongated Galactic orbits and low values of the velocity component in the direction of Galactic rotation, $V_{\rm LSR} \lesssim -200$ km s$^{-1}$. Furthermore, Nissen & Schuster (1997) have shown that these 'metal-rich' halo stars have lower ratios between the $\alpha$-elements and Fe than disk stars in the same metallicity range. As seen from Fig. 6 panel d) there is, however, no systematic differences between the Li abundance of stars with halo and disk kinematics, respectively. Still, we cannot exclude variations in Li/Fe on Galactic scales that are not reflected in the kinematics of the stars. The fact that Be abundances of disk main sequence stars with $T_{\rm eff}$ between 5700 and 6400 K show a large spread (Boesgaard & King 1993) suggests inefficient mixing of light elements produced by cosmic rays considering that beryllium is more robust against stellar destruction than lithium and is unlikely to be depleted in the temperature range mentioned.

The low-Li stars (not included in Fig. 6) can be divided into two classes: lower mass stars with $\log\varepsilon(\rm Li) \lesssim 1.5$ to which the Sun belongs, and higher mass stars originating from a Hyades-like Li dip. For the lower mass, Li-poor stars we note that adding them to Fig. 6 greatly increases the dispersion in Li at the lower mass end of the plots. For the Li-dip stars a tight correlation between metallicity and mass is found (see Fig. 8). A least squares fit to the data gives the following relation

$$M = (1.40 + 0.28[\rm Fe/H])M_\odot \qquad (2)$$

with a dispersion that can be fully explained by the estimated errors in [Fe/H] and mass. Clearly, the special depletion of Li associated with the Hyades-like Li-dip occurs within a narrow mass range at a given metallicity.

It is noted that an extrapolation of Eq. 2 leads to a Li-dip mass of about $1M_\odot$ at [Fe/H] $\simeq -1.5$. This is well above the maximum turnoff mass of halo stars ($\sim 0.8M_\odot$) suggesting that Li-dip stars are unlikely to occur among halo stars at their typical metallicity of [Fe/H] $\simeq -1.5$.

## 5. Conclusions

On the basis of high precision determinations of Li abundance and stellar parameters for a sample of 185 main-sequence field stars with $5600 \lesssim T_{\rm eff} \lesssim 6600$ K and $-1.4 \lesssim$ [Fe/H] $\lesssim +0.2$, two kinds of Li depletion emerge: the as yet unknown process responsible for the Li-dip stars, and the mass dependent depletion of Li, which occurs near the bottom of the convective zone due to destruction of Li by reactions with protons. The group of Li-dip stars is clearly separated from the high-Li stars in the $\log\varepsilon(\rm Li) - T_{\rm eff}$ diagram with a gap of at least 1 dex in the Li abundance.

As shown in Fig. 8 there is a well defined relation between the mass of the Li-dip stars and their metallicity confirming previous findings by Balachandran (1990) and Randich et al. (1999). The derived mass-[Fe/H] relation, Eq. (2), may be used as a constraint on the various stellar mixing theories suggested as an explanation of the Li-dip stars: microscopic diffusion, mass loss, meridional circulation, turbulence or rotational braking; see e.g. the discussion by Balachandran (1995), the study of Talon & Charbonnel (1998), and the recent review by Deliyannis et al. (2000).

Excluding the Li-dip stars, a correlation between Li abundance and stellar mass is found (see Fig. 6), which is probably due to an increasing degree of Li depletion as the outer convection zone deepens with decreasing stellar mass. The dispersion around the Li-mass relation is, however, much larger than expected from observational errors and the residuals are not correlated with stellar age, which for the present sample of stars ranges from $\sim 1.5$ Gyr to about 15 Gyr. This suggests that the main part of Li depletion occurs when the star is young and that other parameters in addition to stellar mass and metallicity affect the degree of depletion, e.g. initial rotation velocity, rate of angular momentum loss or magnetic field strength. Binarity may also play a role for the degree of Li depletion, as exemplified by the two 'intermediate-mass' Li-poor stars HD 80218 and HD 106516A, and although we have excluded double-lined spectroscopic binaries from our sample, a significant fraction of the stars may be binaries with a low mass component. Furthermore, it cannot be excluded that a cosmic scatter of the Li abundance in the Galaxy at a given metallicity contributes to the dispersion in Li abundance, although we have not found any correlation between stellar kinematics and Li abundance.

If the upper envelope of the $\log\varepsilon(\mathrm{Li})$ – [Fe/H] distribution is assumed to represent the Galactic evolution of Li, then the Galactic evolutionary models of Romano et al. (1999) suggest that novae, massive AGB stars, SNeII and Galactic cosmic rays all contribute to the production of Li. In particular, novae seem to provide a major contribution to the Li enrichment and to be responsible for the steep increase of the Li abundance at $[\mathrm{Fe/H}] \simeq -0.4$. It is, however, doubtful if stellar Li abundances along the upper envelope of the $\log\varepsilon(\mathrm{Li})$ – [Fe/H] distribution, based on samples of long-lived F & G stars in this and other works, really represent the Galactic evolution of Li given that there may be a dispersion of Li in the interstellar medium at a given metallicity and that no stars reach the meteoritic Li abundance at solar metallicity. To progress on this problem one will probably need a sample of stars that is an order of magnitude larger than the present sample. Furthermore, it would be interesting to observe the spectra of these stars with higher resolution, say $R \simeq 100\,000$, and very high S/N in order to be able to estimate stellar rotation velocities and magnetic field strengths from the profiles of Zeeman-insensitive and Zeeman-sensitive spectral lines. This would enable a study of possible correlations between the degree of Li depletion and stellar rotation as well as magnetic field strength.

## Acknowledgements

This research was supported by the Danish Research Academy, the Danish Daloon Foundation, the Chinese NSF, and NKBRSF G1999075406.

## References

Alonso A., Arribas S., & Martínez-Roger C. 1996, A&A, 313, 873
Balachandran S. 1990, ApJ, 354, 310
Balachandran S. 1995, ApJ, 446, 203
Boesgaard A.M., & King J.R. 1993, AJ, 106, 2309
Boesgaard A.M., & Tripicco M.J. 1986, ApJ, 302, L49
Boesgaard A.M., & Budge K.G. 1988, ApJ, 332, 410
Carlsson M., Rutten R.J., Bruls J.H.M.J., & Shchukina N.G. 1994, A&A, 288, 860
Chen Y.Q., Nissen P.E., Zhao G., Zhang H.W., & Benoni T. 2000, A&AS, 141, 491
Crawford D.L., & Perry C.L. 1966, AJ, 71, 206
Deliyannis C.P., Pinsonneault M.H., & Charbonnel C. 2000, in Proceedings of IAU Symp. 198 'The light elements and their evolution', ed. L. da Silva, M. Spite, & J.R. de Medeiros, (ASP, San Francisco), 61
Edvardsson B., Andersen J., Gustafsson B., Lambert D.L., Nissen P.E., & Tomkin J. 1993, A&A, 275, 101
ESA 1997, The Hipparcos and Tycho Catalogues, ESA SP-1200
Fuhrmann K., & Bernkopf J. 1999, A&A, 347, 897
Gontcharov G.A., Andronova A.A., & Titov O.A. 2000, A&A, 355, 1164
Jones B.F., Fischer D., & Soderblom D.R. 1999, AJ, 117, 330
Lambert D.L., Heath J.E., & Edvardsson B. 1991, MNRAS, 253, 610
Nissen P.E., & Schuster W.J. 1997, A&A, 326, 751
Nissen P.E., Lambert D.L., Primas F., & Smith V.V. 1999, A&A, 348, 211
Pasquini L. 2000, in Proceedings of IAU Symp. 198 'The light elements and their evolution', ed. L. da Silva, M. Spite, & J.R. de Medeiros, (ASP, San Francisco) , 269
Pasquini L., Liu Q., & Pallavicini R. 1994, A&A ,287, 191
Perryman M.A.C. et al. 1998, A&A, 331, 81
Randich S., Gratton R., Pallavicini R., Pasquini L., & Caretta E. 1999, A&A, 3 48, 487
Rebolo R., Molaro P., & Beckman J.E. 1988, A&A, 192, 192
Romano D., Matteucci F., Molaro P., & Bonifacio P. 1999, A&A, 352, 117
Ryan S.G., Norris J.E., & Beers T.C. 1999, AJ, 523, 654
Sansonetti C.J., Richou B., Engleman R.Jr., & Radziemski L.J. 1995, Phys. Rev. A52, 2682
Smith V.V., Lambert D.L., & Nissen P.E. 1998, ApJ, 506, 405
Spite F., & Spite M. 1982, A&A , 115, 357
Spite M., Francois P., Nissen P.E., & Spite F. 1996, A&A , 307, 172
Steenbock W., & Holweger H. 1984, A&A, 130, 319
Talon S., & Charbonnel C. 1998, A&A, 335, 959
Thorburn J.A., Hobbs L.M., Deliyannis C.P., & Pinsonneault M.H. 1993, ApJ, 415, 150
VandenBerg D.A., Swenson F.J., Rogers F.J., Iglesias C.A., & Alexander D.R. 2000, ApJ, 532, 430
Yan Z.-C., & Drake G.W.F. 1995, Phys. Rev. A52, R4316

**Table 1.** Atmospheric parameters, absolute magnitude, mass, age, equivalent width of the λ6708 Li line, and non-LTE Li abundance. For the majority of stars $M_V$ has been derived from Hipparcos parallaxes but in a few cases (marked by :) a photometric $M_V$ derived from the $c_1$ index is given. Most stellar ages have errors of ≃20% but those marked with ':' are more uncertain, and for stars close to the ZAMS no age is given

| Star<br>HD | $T_{\rm eff}$<br>K | log$g$ | $[\frac{\rm Fe}{\rm H}]$ | $M_V$ | Mass<br>$M_\odot$ | Age<br>Gyr | E.W.<br>mÅ | log $\varepsilon$<br>(Li) |
|---|---|---|---|---|---|---|---|---|
| 400 | 6122 | 4.13 | −0.23 | 3.59 | 1.20 | 4.3 | 26.9 | 2.25 |
| 693 | 6163 | 4.11 | −0.38 | 3.53 | 1.18 | 4.8 | 38.2 | 2.44 |
| 2454 | 6418 | 4.09 | −0.37 | 3.26 | 1.32 | 3.3: | <4.0 | <1.60 |
| 3454 | 6056 | 4.29 | −0.59 | 4.13 | 0.95 | 9.1 | 58.6 | 2.58 |
| 3567 | 6041 | 4.01 | −1.20 | 4.07: | 0.82 | 13.7 | 45.4 | 2.40 |
| 4614 | 5806 | 4.33 | −0.31 | 4.57 | 1.00 | 8.0 | 24.0 | 1.97 |
| 4813 | 6146 | 4.34 | −0.15 | 4.23 | 1.06 | 3.8 | 71.0 | 2.74 |
| 5750 | 6223 | 4.21 | −0.44 | 3.86: | 1.05 | 6.0 | 45.7 | 2.56 |
| 6834 | 6295 | 4.12 | −0.73 | 3.45 | 1.04 | 6.3 | 10.3 | 1.90 |
| 6840 | 5860 | 4.03 | −0.45 | 3.71: | 1.07 | 7.2 | 65.8 | 2.50 |
| 7439 | 6419 | 4.13 | −0.32 | 3.21 | 1.33 | 2.8: | <4.0 | <1.60 |
| 7476 | 6486 | 3.91 | −0.24 | 2.49 | 1.42 | 2.6: | 32.8 | 2.58 |
| 9826 | 6110 | 4.13 | 0.09 | 3.48 | 1.33 | 3.3 | 33.9 | 2.35 |
| 10307 | 5776 | 4.13 | −0.05 | 4.45 | 0.99 | 9.1 | 19.7 | 1.86 |
| 11007 | 6027 | 4.20 | −0.16 | 3.61 | 1.18 | 4.9 | 51.7 | 2.50 |
| 11592 | 6232 | 4.18 | −0.41 | 3.66 | 1.10 | 5.5 | 28.0 | 2.33 |
| 13555 | 6366 | 4.03 | −0.32 | 2.84 | 1.42 | 2.8: | 71.0 | 2.88 |
| 15335 | 5785 | 3.92 | −0.22 | 3.45 | 1.09 | 7.0 | 57.9 | 2.39 |
| 15798 | 6385 | 3.92 | −0.25 | 2.68 | 1.40 | 2.8: | 85.1 | 2.99 |
| 16673 | 6170 | 4.35 | 0.02 | 4.13 | 1.16 | 2.2 | 112.8 | 3.01 |
| 16895 | 6219 | 4.27 | −0.02 | 3.86 | 1.20 | 2.5 | 74.3 | 2.81 |
| 17288 | 5700 | 4.38 | −0.88 | 5.46: | 0.80 |  | 8.3 | 1.41 |
| 17820 | 5750 | 4.11 | −0.69 | 4.52: | 0.83 | 16.4 | 5.6 | 1.28 |
| 18768 | 5695 | 3.91 | −0.62 | 3.40 | 1.09 | 6.8 | 67.7 | 2.43 |
| 19373A | 5867 | 4.01 | 0.03 | 3.94 | 1.09 | 5.7 | 51.2 | 2.38 |
| 22484 | 5915 | 4.03 | −0.13 | 3.61 | 1.08 | 6.3 | 49.1 | 2.39 |
| 22879 | 5790 | 4.28 | −0.84 | 4.76 | 0.78 | 18.8 | 7.8 | 1.45 |
| 24339 | 5810 | 4.20 | −0.67 | 4.43: | 0.86 | 14.4 | 21.9 | 1.94 |
| 24421 | 5986 | 4.10 | −0.37 | 3.81 | 1.03 | 7.9 | 59.7 | 2.54 |
| 25173 | 5867 | 4.07 | −0.62 | 3.52 | 0.99 | 7.9 | 63.3 | 2.49 |
| 25457 | 6162 | 4.28 | −0.11 | 3.95 | 1.16 | 3.5 | 104.5 | 2.95 |
| 25704 | 5765 | 4.12 | −0.91 | 4.81 | 0.78 | 18.7 | 21.6 | 1.90 |
| 25998 | 6147 | 4.35 | −0.11 | 3.82 | 1.16 | 4.2 | 85.3 | 2.82 |
| 28620 | 6101 | 4.08 | −0.52 | 3.61 | 1.09 | 6.1 | 38.2 | 2.40 |
| 30649 | 5695 | 4.24 | −0.51 | 4.58 | 0.88 | 14.5 | <2.0 | <0.80 |
| 33256 | 6385 | 4.10 | −0.30 | 3.12 | 1.32 | 3.3: | <3.0 | <1.40 |
| 33632A | 5962 | 4.30 | −0.23 | 4.40 | 1.06 | 6.0 | 52.3 | 2.45 |
| 34411A | 5773 | 4.02 | 0.01 | 4.20 | 1.01 | 9.4 | 27.4 | 2.02 |
| 35296A | 6015 | 4.24 | −0.14 | 4.15 | 1.00 | 7.5 | 106.4 | 2.87 |
| 38393A | 6306 | 4.29 | −0.07 | 3.83 | 1.21 | 2.6 | 63.5 | 2.79 |
| 39587 | 5805 | 4.29 | −0.18 | 4.72 | 0.90 | 10.7 | 105.6 | 2.71 |
| 39833 | 5767 | 4.06 | 0.04 | 4.30 | 1.00 | 9.4 | 61.7 | 2.40 |
| 41330 | 5791 | 4.10 | −0.24 | 4.01 | 0.98 | 9.3 | 21.9 | 1.92 |
| 41640 | 6004 | 4.37 | −0.62 | 4.58 | 0.95 | 7.2 | 54.7 | 2.51 |
| 43042 | 6485 | 4.27 | 0.04 | 3.58 | 1.30 | 1.1 | 6.0 | 1.82 |
| 43947 | 5859 | 4.23 | −0.33 | 4.41 | 0.98 | 9.8 | 47.0 | 2.33 |
| 46317 | 6216 | 4.29 | −0.24 | 3.80 | 1.19 | 3.7 | 56.6 | 2.67 |
| 49732 | 6260 | 4.15 | −0.70 | 3.73 | 1.04 | 6.3 | 29.7 | 2.37 |
| 51530 | 6017 | 3.91 | −0.56 | 2.82 | 1.28 | 3.4 | <3.0 | <1.20 |
| 54717 | 6350 | 4.26 | −0.44 | 3.86 | 1.10 | 4.6 | 24.2 | 2.34 |
| 55575 | 5802 | 4.36 | −0.36 | 4.44 | 1.00 | 10.6 | 13.5 | 1.71 |
| 58551 | 6149 | 4.22 | −0.54 | 4.09 | 1.04 | 5.9 | 44.0 | 2.49 |
| 58855 | 6286 | 4.31 | −0.31 | 3.87 | 1.16 | 3.6 | 20.3 | 2.22 |
| 59380 | 6280 | 4.27 | −0.17 | 3.64 | 1.20 | 4.2 | 18.1 | 2.16 |
| 59984A | 5900 | 4.18 | −0.71 | 3.55 | 0.99 | 7.8 | 47.3 | 2.36 |
| 60319 | 5867 | 4.24 | −0.85 | 4.37 | 0.80 | 17.0 | 21.2 | 1.96 |
| 61421 | 6671 | 4.02 | −0.02 | 2.65 | 1.50 | 2.1: | <2.0 | <1.40 |
| 62301 | 5837 | 4.23 | −0.67 | 4.07 | 0.90 | 12.2 | 26.2 | 2.04 |
| 63077 | 5831 | 4.19 | −0.78 | 4.45 | 0.80 | 13.6 | 6.1 | 1.37 |
| 63333 | 6057 | 4.23 | −0.39 | 3.92 | 1.03 | 7.5 | 36.3 | 2.35 |
| 68146A | 6227 | 4.16 | −0.09 | 3.77 | 1.10 | 4.9 | 38.6 | 2.49 |
| 68284 | 5832 | 3.91 | −0.56 | 3.41 | 1.09 | 6.4 | 54.4 | 2.39 |
| 69897 | 6243 | 4.28 | −0.28 | 3.85 | 1.19 | 3.3 | 62.7 | 2.73 |
| 70110 | 5949 | 3.96 | 0.07 | 3.12 | 1.40 |  | 55.8 | 2.48 |
| 72945A | 6202 | 4.18 | 0.00 | 3.83 | 1.20 | 2.8 | 105.9 | 2.99 |
| 74011 | 5693 | 4.05 | −0.65 | 4.08 | 0.91 | 12.6 | 18.6 | 1.79 |
| 75332 | 6130 | 4.32 | 0.00 | 3.96 | 1.15 | 3.9 | 106.4 | 2.94 |
| 76349 | 6004 | 4.21 | −0.49 | 3.88 | 1.02 | 8.1 | 46.4 | 2.42 |
| 76932 | 5873 | 4.12 | −0.91 | 4.17 | 0.87 | 12.5 | 26.0 | 2.06 |
| 78418A | 5625 | 3.98 | −0.26 | 3.48 | 1.19 | 5.9 | 33.7 | 2.03 |
| 79028 | 5874 | 4.06 | −0.05 | 3.71 | 0.95 | 7.4 | 76.5 | 2.59 |
| 80218 | 6092 | 4.14 | −0.28 | 3.65 | 1.18 | 4.9 | <2.0 | <1.00 |
| 82328 | 6302 | 3.91 | −0.20 | 2.53 | 1.40 | 2.8: | 112.5 | 3.10 |
| 83220 | 6470 | 4.06 | −0.49 | 3.52 | 1.20 | 5.1 | <3.0 | <1.50 |
| 86560 | 5845 | 4.13 | −0.48 | 4.06 | 0.98 | 9.4 | 31.7 | 2.13 |
| 89125A | 6038 | 4.25 | −0.36 | 4.03 | 1.07 | 6.5 | 40.2 | 2.38 |
| 90839A | 6051 | 4.36 | −0.18 | 4.30 | 1.03 | 5.2 | 60.5 | 2.59 |
| 91347 | 5808 | 4.35 | −0.48 | 4.72 | 0.90 | 10.8 | 24.0 | 1.98 |
| 91752 | 6483 | 4.02 | −0.23 | 2.95 | 1.31 | 2.9: | <2.0 | <1.30 |
| 91889A | 6020 | 4.15 | −0.24 | 3.76 | 1.15 | 5.8 | 44.6 | 2.42 |
| 94280 | 6063 | 4.10 | 0.06 | 3.96 | 1.13 | 4.8 | 52.1 | 2.53 |
| 95128 | 5731 | 4.16 | −0.12 | 4.31 | 0.92 | 12.1 | 18.0 | 1.79 |
| 95241 | 5808 | 3.91 | −0.30 | 2.74 | 1.40 | 3.3 | <1.0 | <0.50 |
| 97916 | 6445 | 4.16 | −0.94 | 3.64: | 1.04 | 5.5 | <5.0 | <1.50 |
| 99747 | 6631 | 4.12 | −0.54 | 3.24 | 1.26 | 2.8 | <5.0 | <1.80 |
| 100180A | 5866 | 4.12 | −0.11 | 4.44 | 0.95 | 9.2 | 57.0 | 2.43 |
| 100446 | 5967 | 4.29 | −0.48 | 4.14 | 0.98 | 8.8 | 29.3 | 2.18 |
| 100563 | 6423 | 4.31 | −0.02 | 3.65 | 1.27 | 1.6 | 48.6 | 2.72 |
| 101676 | 6102 | 4.09 | −0.47 | 3.64 | 1.09 | 6.1 | 35.1 | 2.36 |
| 102634 | 6333 | 4.22 | 0.24 | 3.48 | 1.35 | 2.3 | 35.9 | 2.53 |
| 102870 | 6068 | 4.09 | 0.13 | 3.41 | 1.32 |  | 15.3 | 1.96 |
| 103723 | 6062 | 4.33 | −0.75 | 4.65: | 0.96 | 4.8 | 35.1 | 2.33 |
| 103799 | 6169 | 4.02 | −0.45 | 3.29 | 1.20 | 4.8 | 21.9 | 2.18 |
| 105004 | 5832 | 4.32 | −0.78 | 5.56 | 0.90 |  | 21.7 | 1.95 |
| 106038 | 5939 | 4.23 | −1.33 | 4.98: | 0.70 | 20.7 | 64.1 | 2.51 |
| 106516A | 6135 | 4.34 | −0.71 | 4.35 | 0.90 | 9.3 | <2.0 | <1.10 |
| 107113 | 6373 | 4.07 | −0.54 | 3.34 | 1.18 | 4.1 | <4.0 | <1.50 |
| 108134 | 5761 | 4.17 | −0.44 | 4.24 | 0.98 | 10.3 | 23.0 | 1.93 |
| 108510 | 5929 | 4.31 | −0.06 | 4.44 | 1.05 | 5.2 | 48.8 | 2.39 |
| 109303 | 5905 | 4.10 | −0.61 | 3.55 | 1.00 | 8.4 | 47.3 | 2.37 |
| 109358 | 5750 | 4.30 | −0.19 | 4.66 | 0.89 | 12.4 | 9.0 | 1.49 |
| 110897 | 5757 | 4.31 | −0.59 | 4.76 | 0.85 | 14.5 | 23.0 | 1.92 |
| 113679 | 5595 | 3.98 | −0.71 | 3.75 | 0.95 | 10.4 | 32.9 | 1.99 |
| 114642A | 6355 | 3.91 | −0.17 | 2.47 | 1.41 | 2.8: | 94.4 | 3.03 |
| 114710A | 5877 | 4.24 | −0.05 | 4.45 | 0.94 | 9.6 | 66.3 | 2.51 |

**Table1.**(continued)

| Star | $T_{\rm eff}$ | $\log g$ | $[\frac{\rm Fe}{\rm H}]$ | $M_V$ | Mass | Age | E.W. | $\log\varepsilon$ |
|---|---|---|---|---|---|---|---|---|
| HD | K | | | | $M_\odot$ | Gyr | mÅ | (Li) |
| 114762 | 5821 | 4.15 | −0.74 | 4.26 | 0.88 | 12.9 | 25.1 | 2.01 |
| 114837 | 6241 | 4.18 | −0.28 | 3.63 | 1.20 | 4.2 | 22.7 | 2.24 |
| 115383A | 5866 | 4.03 | 0.00 | 3.92 | 1.09 | 5.7 | 84.6 | 2.64 |
| 118244 | 6234 | 4.13 | −0.55 | 3.71 | 1.07 | 5.8 | 16.0 | 2.07 |
| 120162 | 5823 | 4.33 | −0.73 | 4.75 | 0.84 | 13.5 | 35.0 | 2.16 |
| 120559 | 5405 | 4.40 | −0.88 | 6.22: | 0.80 | | <2.0 | <1.00 |
| 121004 | 5622 | 4.31 | −0.71 | 4.72: | 0.80 | 18.3 | <4.0 | <1.00 |
| 121560 | 6059 | 4.35 | −0.38 | 4.24 | 1.00 | 7.1 | 41.1 | 2.40 |
| 124244 | 5853 | 4.11 | 0.05 | 3.57 | 1.19 | 5.8 | 51.9 | 2.37 |
| 126512 | 5714 | 4.02 | −0.63 | 3.92 | 0.97 | 10.1 | 18.6 | 1.81 |
| 126681 | 5533 | 4.28 | −1.14 | 5.59: | 0.70 | 17.5 | 14.9 | 1.54 |
| 127334 | 5501 | 4.16 | 0.05 | 4.52 | 0.90 | 15.9 | 16.4 | 1.60 |
| 128167 | 6737 | 4.25 | −0.41 | 3.53 | 1.30 | 1.0: | <3.0 | <1.60 |
| 128385 | 6041 | 4.12 | −0.33 | 4.26 | 1.06 | 5.5 | 31.0 | 2.26 |
| 130551 | 6274 | 4.19 | −0.72 | 3.77 | 1.07 | 7.6 | 28.2 | 2.36 |
| 130948 | 5780 | 4.18 | −0.20 | 4.61 | 0.97 | 10.0 | 103.1 | 2.69 |
| 131117 | 6014 | 4.00 | 0.13 | 3.17 | 1.40 | | 73.2 | 2.67 |
| 132254 | 6231 | 4.22 | 0.07 | 3.64 | 1.23 | 3.2 | 35.4 | 2.45 |
| 136351 | 6343 | 3.91 | 0.01 | 2.32 | 1.62 | | 37.6 | 2.56 |
| 139457 | 5941 | 4.06 | −0.52 | 3.70 | 0.98 | 8.7 | 48.8 | 2.41 |
| 141004 | 5801 | 4.16 | −0.04 | 4.07 | 1.04 | 8.4 | 23.0 | 1.95 |
| 142373 | 5920 | 4.27 | −0.39 | 3.61 | 0.96 | 9.7 | 61.5 | 2.51 |
| 142860A | 6227 | 4.18 | −0.22 | 3.63 | 1.20 | 4.2 | 19.0 | 2.15 |
| 143761 | 5698 | 4.14 | −0.26 | 4.20 | 0.99 | 11.2 | 6.0 | 1.28 |
| 146099A | 5941 | 4.10 | −0.61 | 3.57 | 1.00 | 8.1 | 45.5 | 2.37 |
| 146588 | 5895 | 4.29 | −0.63 | 4.53 | 0.90 | 11.0 | 42.6 | 2.31 |
| 149750 | 5792 | 4.17 | 0.08 | 4.05 | 1.11 | 7.5 | 30.6 | 2.07 |
| 150453 | 6458 | 3.91 | −0.37 | 2.41 | 1.51 | 2.3: | 32.8 | 2.56 |
| 154417 | 5925 | 4.30 | −0.04 | 4.47 | 1.05 | 5.0 | 80.5 | 2.65 |
| 155358 | 5818 | 4.09 | −0.67 | 4.09 | 0.89 | 12.7 | 23.0 | 1.97 |
| 157347 | 5654 | 4.36 | −0.02 | 4.84 | 1.06 | 7.7 | <5.0 | <1.10 |
| 157466 | 5935 | 4.32 | −0.44 | 4.51 | 0.95 | 8.4 | 46.7 | 2.38 |
| 159332 | 6204 | 3.91 | −0.23 | 2.82 | 1.29 | 3.3: | <4.0 | <1.50 |
| 160291 | 6008 | 4.10 | −0.53 | 3.78 | 1.04 | 7.5 | 28.4 | 2.20 |
| 162004B | 6059 | 4.12 | −0.08 | 4.03 | 1.10 | 5.6 | 65.9 | 2.64 |
| 165908 | 6083 | 4.19 | −0.56 | 3.98 | 1.04 | 6.8 | 38.2 | 2.39 |
| 167588 | 5894 | 4.13 | −0.33 | 3.45 | 1.18 | 4.9 | 46.5 | 2.35 |
| 168009 | 5719 | 4.08 | −0.07 | 4.52 | 0.89 | 12.8 | <4.0 | <1.10 |
| 168151 | 6529 | 4.15 | −0.31 | 3.17 | 1.35 | 2.5 | <2.0 | <1.40 |
| 170153A | 6034 | 4.28 | −0.65 | 4.04 | 0.95 | 9.4 | 36.0 | 2.32 |
| 174912 | 5787 | 4.35 | −0.54 | 4.77 | 0.87 | 13.8 | 32.8 | 2.11 |
| 184601 | 5830 | 4.20 | −0.81 | 4.48: | 0.80 | 17.1 | 40.7 | 2.24 |
| 186379 | 5816 | 3.99 | −0.46 | 3.60 | 1.10 | 7.0 | 44.8 | 2.29 |
| 187691 | 6034 | 4.16 | 0.09 | 3.69 | 1.23 | 4.5: | 69.9 | 2.65 |
| 189340 | 5888 | 4.26 | −0.19 | 3.93 | 0.96 | 9.4 | 46.0 | 2.34 |
| 191862A | 6328 | 4.19 | −0.27 | 3.61 | 1.15 | 5.9 | 62.9 | 2.79 |
| 198390 | 6339 | 4.20 | −0.31 | 3.62 | 1.20 | 3.8 | 17.0 | 2.17 |
| 199960 | 5750 | 4.17 | 0.11 | 4.10 | 1.09 | 8.3 | 59.0 | 2.37 |
| 200580 | 5829 | 4.39 | −0.58 | 3.58 | 0.87 | 13.3 | 22.9 | 1.97 |
| 201891 | 5827 | 4.43 | −1.04 | 4.64 | 0.70 | 21.7 | 25.5 | 2.01 |
| 203608 | 6109 | 4.34 | −0.67 | 4.41 | 0.95 | 7.2 | 37.3 | 2.39 |
| 204306 | 5896 | 4.09 | −0.65 | 3.74 | 0.98 | 8.9 | 44.1 | 2.33 |
| 204363 | 6141 | 4.18 | −0.49 | 3.89 | 1.06 | 6.3 | 73.3 | 2.75 |
| 206301 | 5682 | 3.98 | −0.04 | 3.68: | 1.09 | 6.7 | 62.1 | 2.35 |
| 206860 | 5798 | 4.25 | −0.20 | 4.66 | 0.97 | 9.9 | 109.5 | 2.73 |
| 208906A | 5929 | 4.39 | −0.73 | 4.62 | 0.83 | 13.6 | 40.7 | 2.31 |

**Table1.**(continued)

| Star | $T_{\rm eff}$ | $\log g$ | $[\frac{\rm Fe}{\rm H}]$ | $M_V$ | Mass | Age | E.W. | $\log\varepsilon$ |
|---|---|---|---|---|---|---|---|---|
| HD | K | | | | $M_\odot$ | Gyr | mÅ | (Li) |
| 209942A | 6022 | 4.25 | −0.29 | 4.00 | 1.10 | 6.2 | 38.5 | 2.35 |
| 210027A | 6496 | 4.25 | −0.17 | 3.41 | 1.23 | 2.7 | 72.0 | 2.98 |
| 210752 | 5847 | 4.33 | −0.68 | 4.56 | 0.85 | 14.0 | 39.0 | 2.23 |
| 212029A | 5875 | 4.36 | −1.01 | 4.70 | 0.76 | 18.8 | 27.9 | 2.08 |
| 215257 | 5976 | 4.36 | −0.65 | 4.28 | 0.90 | 11.2 | 38.3 | 2.31 |
| 216385 | 6244 | 3.97 | −0.25 | 3.02 | 1.29 | 3.3: | <2.0 | <1.20 |
| 218470 | 6495 | 4.06 | −0.13 | 3.04 | 1.32 | 2.6: | <4.0 | <1.70 |
| 219476 | 5887 | 3.91 | −0.59 | 2.78 | 1.27 | 3.4 | <2.0 | <0.90 |
| 219623A | 6039 | 4.07 | 0.02 | 4.04 | 1.10 | 5.5 | 68.0 | 2.65 |
| 221377 | 6348 | 3.91 | −0.96 | 2.80 | 1.13 | 4.5 | <3.0 | <1.40 |
| 222368 | 6169 | 4.06 | −0.17 | 3.43 | 1.15 | 4.8 | 20.8 | 2.16 |
| 241253 | 5830 | 4.23 | −1.10 | 5.36: | 0.76 | 10.8 | 29.5 | 2.08 |
| BD-21 3420 | 5858 | 4.25 | −1.09 | 5.08: | 0.72 | 19.2 | 21.5 | 1.95 |
| CD-33 3337 | 6022 | 3.99 | −1.34 | 4.16: | 0.77 | 16.4 | 38.0 | 2.32 |
| CD-45 3283 | 5650 | 4.50 | −0.84 | 5.71: | 0.80 | | <2.0 | <0.70 |
| CD-47 1087 | 5657 | 4.20 | −0.80 | 5.08: | 0.74 | 22.7 | 5.7 | 1.21 |
| CD-57 1633 | 5944 | 4.22 | −0.89 | 5.12: | 0.90 | | 33.7 | 2.22 |
| CD-61 0282 | 5772 | 4.20 | −1.23 | 5.27: | 0.70 | 18.6 | 34.8 | 2.12 |
| G005-040 | 5737 | 4.02 | −0.91 | 4.76: | 0.77 | 19.5 | 10.1 | 1.90 |
| G046-031 | 5907 | 4.18 | −0.81 | 5.12: | 0.88 | | 26.8 | 2.09 |
| G088-040 | 5911 | 4.14 | −0.83 | 4.60: | 0.83 | 13.8 | 24.6 | 2.06 |
| G102-020 | 5310 | 4.56 | −1.09 | 6.00: | 0.70 | | 7.1 | 1.26 |
| W7547 | 6272 | 4.03 | −0.42 | 3.27: | 1.25 | | <2.0 | <1.20 |